# Heat Transport and Temperature Distributions in Large Single Drops at Low Reynolds Numbers: A New Experimental Technique

**HARLAN N. HEAD and J. D. HELLUMS**

**Rice University, Houston, Texas**

**A new experimental technique has been developed for study of transport from drops. Large single drops are heated dielectrically while suspended motionless in an unheated continuous phase. Direct measurements of temperature distributions within drops are presented both for circulating drops and for drops in which surface-active materials retard circulation. The results of the measurements will be useful in assessing the validity of the various proposed models.**

The prediction of transport rates from a drop freely falling or rising in a second immiscible liquid is complicated because of the hydrodynamics of the moving drop. Bulk heat transport coefficients have been measured by several investigators (*1, 3, 8*) by letting drops of hot disperse liquid fall through a continuous fluid and then gathering the drops and measuring the heat lost from the disperse liquid. In these experiments the measured rates of heat transport depended extensively on drop forming and collecting techniques and the measurements were inherently at unsteady state conditions.

In the investigation reported here a new experimental technique was developed to provide information that supplements the previous work. In these experiments large single drops were suspended in a continuous phase liquid flowing up through a tapered tube and heated indirectly by high-frequency dielectric power. By this means a stationary drop could be heated and allowed to cool under controlled conditions. This technique eliminates the problems associated with drop formation and coalescence and eliminates the need for interpretation of overall measurements of mixed mean temperature or concentration.

Rates of heat transfer from drops were obtained by measuring the temperature rise in the continuous phase liquid as it passed the drop. The actual temperature distributions within cooling drops were obtained by use of a fine thermocouple probe. Both drops with full internal circulation and drops with retarded circulation were investigated. The investigation was limited to low Reynolds numbers in which flow was laminar with no boundary-layer separation from the drop and to high Peclet numbers in which the bulk of the thermal resistance was in the continuous phase.

## BRIEF REVIEW OF THEORY

Different expressions can be developed for the transport of energy within a drop depending upon the type of internal motion that is assumed.

The solution for diffusion in a solid sphere initially at a uniform temperature whose surface temperature is suddenly lowered is

$$H(t)/H(o) = 6 \sum_{n=1}^{\infty} B_n \exp(-\gamma_n^2 t^*) \qquad (1)$$

A completely mixed drop cooling in a continuous phase has a uniform internal temperature for all time. In this case a simple energy balance gives the cooling relationship

$$H(t)/H(o) = \exp\left(-\frac{3}{2}\frac{hD}{k_d}t^*\right) \qquad (2)$$

An analytical solution for transport in a drop rising or falling in slow viscous motion was developed by Kronig and Brink (*6*). This solution was based on the Hadamard stream function (*7*):

$$\psi_d = \frac{-g(\rho_d - \rho_c)a^2}{6(2\mu_c + 3\mu_d)}\left(\frac{r^2}{a^2}\right)\sin^2\theta \qquad (3)$$

which describes the internal motion of a slowly moving drop. If the rate of diffusion of energy is sufficiently small, then the streamlines and isotherms within the drop will coincide. By making this assumption the transport problem is reduced to one of energy diffusion normal to the Hadamard streamlines. The solution developed by Kronig and Brink for this case is

$$H(t)/H(o) = \frac{3}{8}\sum_{n=1}^{\infty} A_n^2 \exp(-16\lambda_n t^*) \qquad (4)$$

The coefficients $A_n$ and eigenvalues $\lambda_n$ are listed by Elzinga and Banchero (*3*) as functions of $hD/k_d$.

Equations presented by Levich (*7*) for the prediction of external transport coefficients are

$$N_{Nu} = 0.65\, N_{Pe}^{1/2}\left(\frac{\mu_c}{\mu_c + \mu_d}\right)^{1/2} \qquad (5)$$

for a drop with full internal circulation and

$$N_{Nu} = 0.998\, N_{Pe}^{1/2} \qquad (6)$$

for a solid sphere. Both of these equations, as well as the Kronig and Brink relationship, are based on assumptions corresponding to the large Prandtl number (Schmidt number for diffusion) asymptote. In addition the interface is assumed to be isothermal.

Harlan N. Head is with Shell Development Company, Emeryville, California.

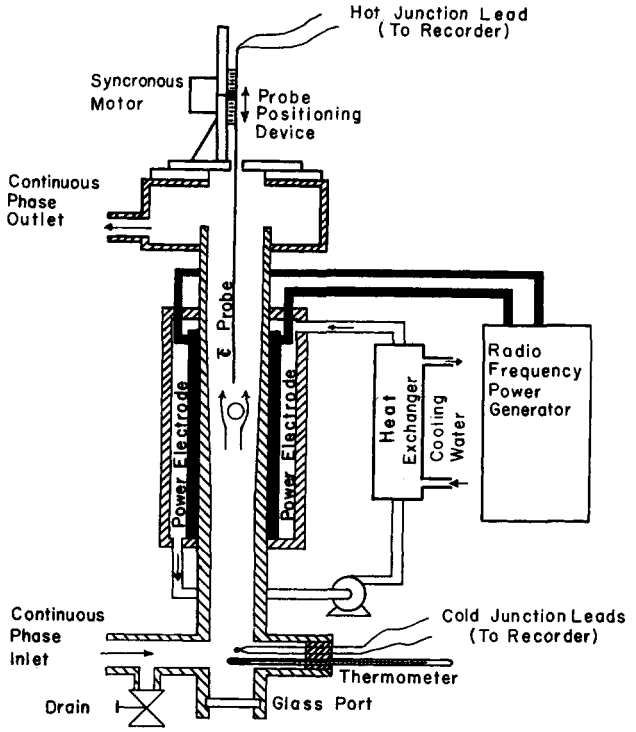


Fig. 1. Diagram of tapered tube assembly.

## EXPERIMENTAL EQUIPMENT

The three basic components of the experimental apparatus used in this investigation were a flow system for supporting a drop in a tapered tube, a system for heating the drop with dielectric power, and a system for measuring temperatures at points in and around the drop.

### Flow System

The tapered tube assembly is shown in Figure 1. The tube was made of polystyrene and was 12 in. long with a 6-in. tapered section in the middle. In the tapered section the tube diameter increased from 1¾ to 2 in., creating a taper of approximately 1¼ deg. The outer diameter of the tube was 2¼ in. The tapered tube assembly could be aligned vertically by means of adjusting screws at its base.

The continuous phase liquid was circulated from a storage tank up through the tapered tube and back to the tank. Air bubbles were removed from the continuous phase liquid before it entered the tapered tube by passing the liquid into a tank and pulling a slight vacuum on it. A drop trap was installed to catch any drop material that might escape from the tapered tube into the circulating system.

Water-glycerol mixtures were used for the drop material, while high viscosity Dow Corning silicone fluids (dimethylpolysiloxane) were used for the continuous phase. The water-glycerol mixtures were only slightly more dense than the silicone fluids and large drops up to ¾ in. in diameter could be formed easily. Drops were deposited in the flowing continuous phase within the tapered tube through a burette with an I.D. at the tip of about ⅜ in. Continuous phase velocities required to support a drop within the tapered tube were in the range of 1 to 2 in./sec.

The vertical position of a drop in the tapered tube could be controlled easily by adjusting the continuous phase flow rate. Keeping a drop centered horizontally in the tube was more difficult. The tube had to be aligned carefully in the vertical direction before a drop would remain centered. Even then under some conditions drops would not center. The continuous phase silicone fluids used in these experiments had viscosities of 103 and 207 centipoise. Drops in these liquids remained centered in the tube and would return to the center if pushed aside. Drops in both 10- and 1,000-centipoise silicone fluids did not remain in the center of the tube but migrated to the wall. Drops formed in the 103- and 207-centipoise fluids with diameters larger than ¾ in. also migrated to the wall. In his photographic study of drop circulation in tapered tubes, Horton (5) also observed that under some conditions drops remained centered, while at other conditions they did not.

Tygon plastic tubing and polystyrene couplings were used in the continuous phase flow system rather than glass, which would have lessened the possibility of surface-active materials being present. This proved to be unfortunate, because impurities from these materials dissolved in the continuous phase fluids in sufficient quantities to retard circulation in even the largest drops formed in these experiments. This is in direct conflict with the statement of Levich (7) that surface-active materials cannot retard the interfacial motion of a relatively large drop. As a result much of the experimental data obtained were from drops with retarded circulation. However, data were obtained for circulating drops at high Peclet numbers by measuring before impurities built up sufficiently at the drop surface to retard circulation. The circulation patterns within the drops were observed in several series of experiments in which fine aluminum oxide particles were suspended in the drop liquid. In newly formed drops the patterns appeared to be qualitatively consistent with the Hadamard solution. However, in about 30 min. to 1 hr. the downstream section of the drop could be observed to have a slightly reduced circulation. The area of retarded circulation gradually grew until after several hours the drop would appear to be entirely stagnant.

### Dielectric Heating System

Dielectric heating utilizes a radio frequency field developed between two electrodes to generate heat within a material. A simple explanation is that molecules having a dipole moment are alternately stressed in opposite directions by the electrical field. This stress is manifested as heat generated within the material.

The fact that high-frequency power heats only dipole materials was utilized to heat the drop suspended in the tapered tube. While the drop materials, water and glycerol, heat readily, the polystyrene tube and the silicone fluid continuous phase are unaffected by a high-frequency field.

For this work a 1-kw. dielectric generator with an operating range of 26.3 to 27.4 megacycles built by Reeve Electronics, Inc., Chicago, was used to produce the high-frequency field. This generator had about a 2,000-v. output which, when coupled to a special tank circuit, was raised to about 10,000 to 15,000 v. The magnitude of power input to the drop could be controlled by tuning the generator.

The flat plate electrodes, made of ⅛ in. silver-plated copper, were placed against the tapered tube on opposite sides as

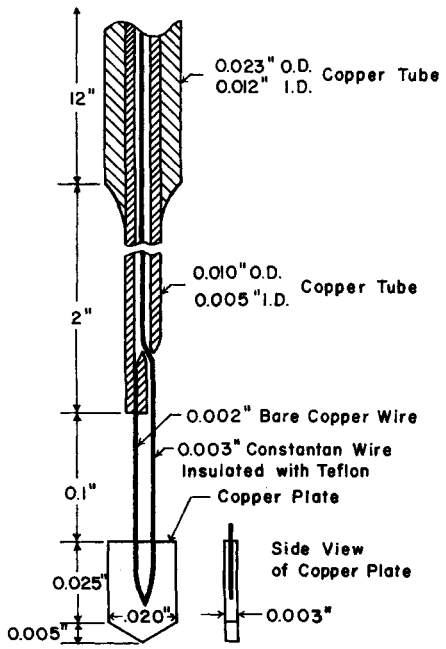


Fig. 2. Diagram of the thermocouple probe tip.

shown in Figure 1. They were designed to produce a uniform field within the drop (*4*). With an electrode spacing of 2¼ in., as used in these experiments, a uniform field was assured in drops up to a maximum diameter of ¾ in.

The surface dimensions of each electrode were 9¼ × 9 in. This was sufficiently large to eliminate the effect on the drop of the field distortion at the edges of the electrodes and to give a 2-in. safety margin on all sides. Originally, electrodes 3½ × 5 in. were installed but they were not satisfactory. When power was turned on to heat a suspended drop, the drop was attracted toward the edge of one of the electrodes. This was caused by the fact that lines of force converge at the edge of an electrode and that neutral particles, in this case, the drop, are attracted in the direction of converging lines of force. This phenomenon, called *dielectrophoresis,* is described by Pohl (*10*).

A second effect caused by the high-frequency field was to elongate the drops in a direction perpendicular to the electrodes. This prolate distortion varied directly with the intensity of the field up to a maximum of major to minor diameters of about 1.3 for the field intensities used in these experiments. When the field was turned off, the drop would immediately return to the spherical shape and there was no evidence that this distortion materially affected the circulation patterns within the drop.

A tank built around the electrode-tapered tube assembly and filled with silicone fluid served two purposes. First, since the polystyrene tube and silicone fluid have similar dielectric properties, it created a homogeneous medium between the electrodes. Second, resistive heat developed in the electrodes by the high electrical currents was carried away by circulating the silicone fluid through a water jacketed cooling coil.

The high-frequency circuit was designed so that a plane of ground potential would exist parallel to the power electrodes and somewhere between them. This plane could be moved in the direction of either of the electrodes by adjusting tubing capacitors in the circuit.

### Temperature Measuring System

A fine copper-constantan thermocouple probe extending down into the tapered tube from above was used to measure the temperatures in and around the drop. The cold junction was located in the continuous phase stream at the base of the tapered tube so that the probe measured temperature differences above that of the continuous phase.

The probe was made as shown in Figure 2 by running a 40-gauge Teflon-insulated constantan wire down a copper tube assembly. Originally a probe was built with the constantan wire extending down the center of the smaller diameter copper tube to its tip where a solder junction was made. This led to inaccurate temperature measurements, because the high thermal conductivity of the copper allowed heat to be conducted away from the tip. Therefore the thermocouple junction was extended beyond the copper tube with a 0.002-in. copper wire. A thin bit of copper plate was attached to the junction to act as a heat sink. With this arrangement the effect of thermal conductivity along the thermocouple wires was minimized.

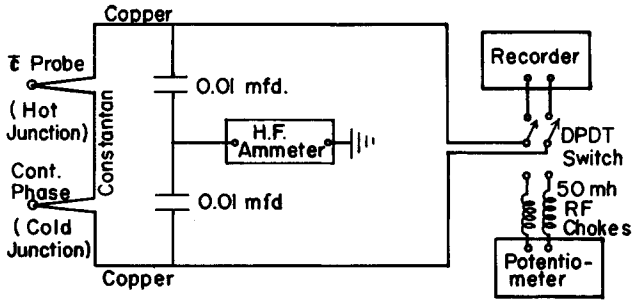


Fig. 3. Schematic diagram of the temperature measuring circuit.

Both the original cylindrical probe and the plate probe were analyzed for error by constructing a conduction model with estimated heat transfer coefficients. The plate probe was found to yield errors of a very few percent, whereas substantial errors were incurred in the cylindrical probe. The plate probe has the disadvantage however of larger dimensions so that temperature measurements are averaged over a larger area.

At the top of the tapered tube the probe was attached to a positioning device which allowed the probe to be set in any position in the horizontal dimensions to within 0.1 mm. The probe was also geared to a synchronous motor so that it could be moved up and down over a distance of 4 in. at any of four speeds. This arrangement allowed temperature profiles to be recorded by positioning the probe above the drop and then moving it down through the drop.

Special precautions were necessary when recording thermal emf measurements within the high-frequency field. It was necessary to adjust the plane of ground potential between the power electrodes to coincide with the thermocouple probe. Otherwise, the probe would provide a path to ground and high-frequency currents flowing through the probe would overpower the thermal emf signal. The temperature measuring circuit is shown in Figure 3. A capacitive path to ground was provided through a high-frequency ammeter. The field around the probe was properly adjusted when no current flowed through the ammeter.

Thermal emf signals were measured by a 1-mv. recorder while the high-frequency power was off and by a potentiometer shielded with R. F. chokes while the high-frequency power

Table 1. Properties of the Two Systems Studied (*2, 9*)

| | Circulating drop system | | Retarded drop system | |
|---|---|---|---|---|
| | Disperse phase | Continuous phase | Disperse phase | Continuous phase |
| Composition | 25 wt. % glycerol in distilled water with 10 p.p.m. methylene blue added for color | 200 centipoise Dow Corning 200 silicone fluid | 10 wt. % glycerol in distilled water with 10 p.p.m. methylene blue added for color | 100 centipoise Dow Corning 200 silicone fluid |
| Drop volume, ml. | 2.1 | | 2.5 | |
| Sphere equivalent drop diameter, in. | 0.63 | | 0.66 | |
| Drop velocity $v$, in./sec. | 1.17 | | 1.04 | |
| Specific gravity | 1.054 | 0.967 | 1.019 | 0.965 |
| $k$, B.t.u./(hr.)(ft.)(°F.) | 0.296 | 0.090 | 0.334 | 0.090 |
| $C_v$, B.t.u./(lb.)(°F.) | 0.89 | 0.33 | 0.96 | 0.33 |
| $\mu$, lb./(ft.)(sec.) | 0.0010 | 0.130 | 0.00066 | 0.061 |
| $\alpha$, sq. in./sec. | $2.02 \times 10^{-4}$ | $1.81 \times 10^{-4}$ | $2.19 \times 10^{-4}$ | $1.81 \times 10^{-4}$ |
| Prandtl number | 11 | 1,700 | 6.8 | 800 |
| Reynolds number | | 2.4 | | 4.8 |
| Peclet number | 3,700 | 4,100 | 3,100 | 3,800 |

was on. The recorder could not be used with the power on because the high-frequency signal would jam the amplifier.

## EXPERIMENTAL MEASUREMENTS

Two systems were studied and compared: one in which the internal circulation of the drop was retarded by surface-active impurities, and the other in which the drop was fully circulating. The physical properties of the two systems are given in Table 1. In these systems the flow was laminar with no boundary-layer separation or turbulence in the wake of the drop, and the bulk of the thermal resistance was in the continuous phase.

A drop deposited in the tapered tube was heated by the high-frequency field until a steady state was reached between the heat generated in the drop and that lost to the continuous phase. The approach to steady state was followed by measuring the peak temperature in the thin column of heated continuous phase rising above the drop. From this steady state situation the drop was allowed to cool by turning off the power. Measurements were taken of the temperature distribution within the drop and also of the temperature decay of the heated column rising from the drop. To obtain a complete set of these measurements it was necessary to heat the drop to an identical steady state several times.

### Temperature Distributions Within the Drops

The measured temperature distributions within the two drop systems are shown in Figures 4 and 5. These figures were constructed from the recorded profiles of vertical passes of the thermocouple probe down through the drop. Because the recorder could not be used with the high-frequency power on, the passes were made immediately after turning off the power. Before each pass the probe was positioned at a given distance above the centerline of the drop and the drop was heated to the steady state. The temperatures are given in °F. above the continuous phase inlet temperature.

A complete set of figures showing temperature distributions at various stages of cooling is presented in reference 4. The complete set shows that the temperature patterns retain approximately the same shape during the entire cooling period. In particular, notice that in the circulating drop there is a region of high temperature, the 5.5°F. closed isotherm in Figure 5, along a vertical diameter of the drop. This relatively high temperature region continued to exist as long as the drop temperature was observed, as temperatures at all points decreased with time. The maximum temperature continued to lie in the same region as shown in Figure 4 to within the accuracy of the measurements.

The drop was forced both downward and sidewise by the movement of the probe through it. Downward movement was about 2 mm., while sidewise movement varied from 0 to about 2 mm., depending on the horizontal distance off center of the probe. In constructing the temperature distribution figures, compensation was made for the sidewise movement of the drop by slanting the lines along which the temperature profiles were plotted. These lines are included in the figures to show how this was done. Temperature measurements near the edges of the drops were difficult to evaluate because of this sidewise movement. The locations of the isotherms for passes through the drop near the center are more accurate than for those near the edge. No direct compensation was made in the figures for the downward movement of the drops but a properly scaled outline of each drop elongated by 2 mm. is shown in the figures as a dashed line. This outline is not precise in location for the reasons given above.

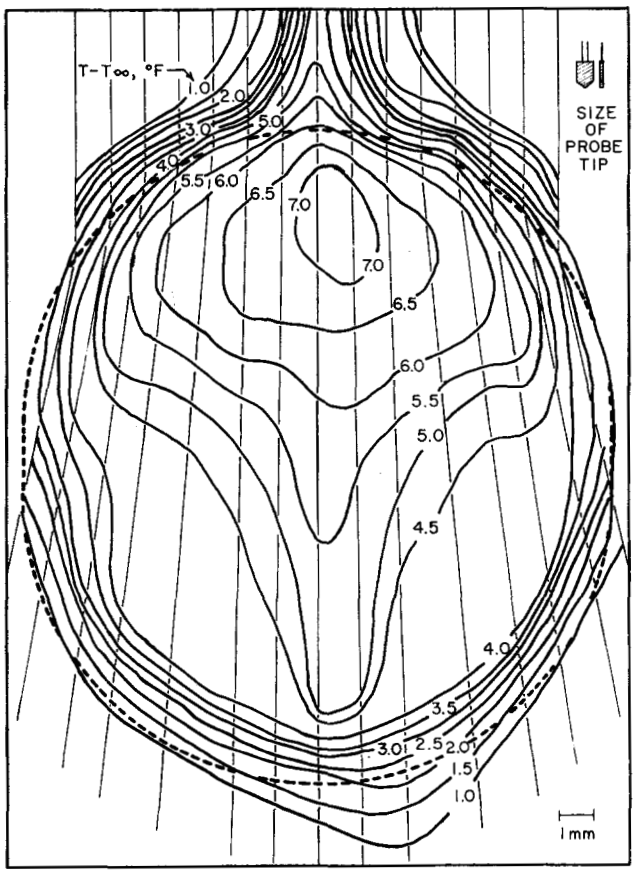


Fig. 4. Isotherms in a drop with retarded circulation.

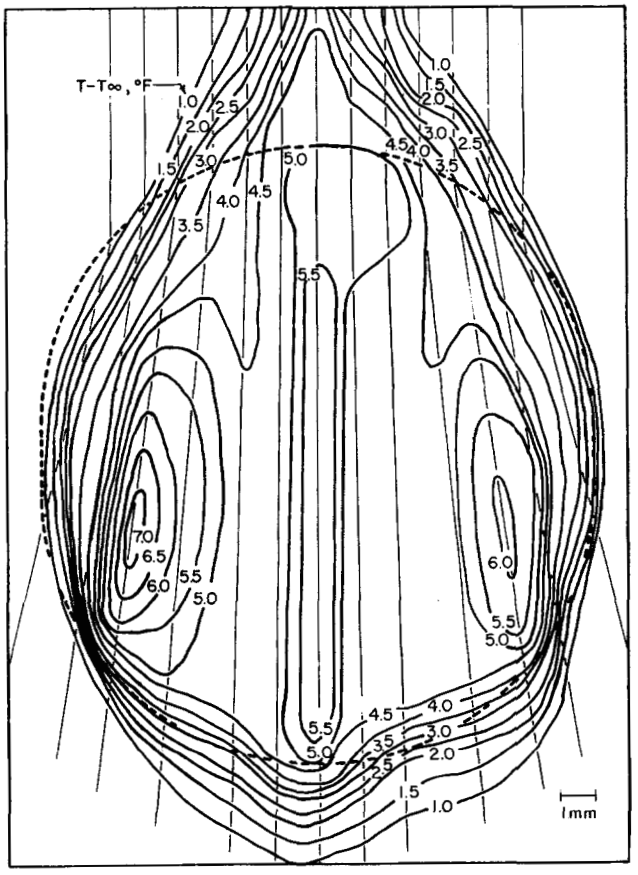


Fig. 5. Isotherms in a drop with full circulation.

At the time the power was turned off the probe tip was 20 and 10 mm. above the center of the drops with retarded and with full circulation, respectively. The probe traveled at 8.15 mm./sec. and the drop diameters were about 16 mm. The time required for the probe to travel from this initial position to the bottom of the drop was about 3½ sec. for the retarded drop and about 2¼ sec. for the circulating drop. Although this measuring time was not negligible, it was small compared to the 2 to 3 min. required for the drop to cool to within 0.5°F. of the continuous phase temperature. Tests on the thermocouple-recorder system indicated a response time of about 0.05 sec.

The effect of internal circulation on the temperature distribution within the drops is apparent from the figures. Some limited circulation is indicated in the retarded drop figure by the uniformity of temperatures in the lower portions of the drop. The slightly higher temperature on the left in the circulating drop figure suggests that the tapered tube was not truly vertical and that a slightly nonsymmetrical circulation pattern existed. The shapes of the isotherms immediately above the drops indicate that no boundary-layer separation or turbulence in the wake occurred.

The average temperatures of these drops were estimated to be between 4.5° and 5°F. above the continuous phase for both the fully circulating and the retarded drops. This estimate was made by measuring the area enclosed by each isotherm in Figures 4 and 5 with a planimeter, evaluating the volume of revolution for each area, and then integrating with the definition of the mixed mean temperature.

The relative size of the temperature sensing tip of the probe is shown in Figure 4. In taking the data, the tip was oriented as indicated in the side view. The dimensions of the sensing surface were 0.020 in. × 0.025 in. These dimensions are on the order of the thickness of the thermal boundary layer surrounding the drop. This excludes the possibility of determining the nature of the temperature gradients within the boundary layer or of measuring precisely the interfacial temperature over much of the surface of the drop. To make such measurements an extremely small sensing device would be required along with a recording instrument with very fast response. Despite this, some definite conclusions about the interfacial temperatures could be made from the temperature distribution data obtained in these experiments. Figure 4 for the retarded drop shows that in the area of the front stagnation point $T_a - T_\infty$ must have been close to 4°F. At the wake $T_a - T_\infty$ must have been 5°F. or higher. For the fully circulating drop Figure 5 shows that $T_a - T_\infty$ was near 4.5°F. in the vicinity of the front stagnation point and that $T_a - T_\infty$ was 4.5°F. or higher at the wake. These figures on the interface temperature must be regarded as semiquantitative in nature. However, the interface determination is accurate enough to show that the isothermal interface idealization used in most analyses is inadequate. It can be seen in Figure 5 that the front and rear stagnation points are several degrees higher in temperature than the interface halfway between.

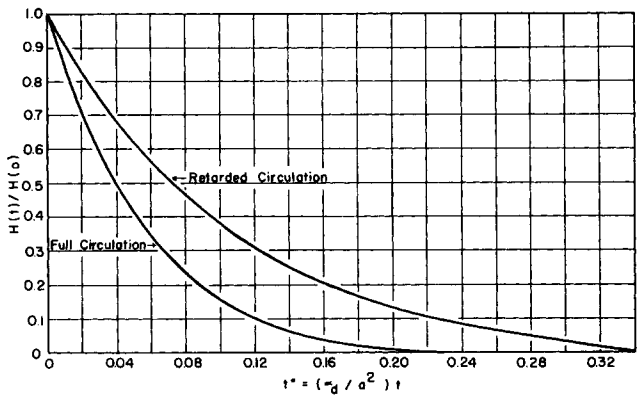


Fig. 6. Experimental cooling curves.

The high temperatures along the vertical axis of the circulating drop were unexpected, especially since this region remained relatively hot during the entire cooling period of the drop. It was anticipated that the region around the vertical axis would be cool because of the circulation pattern. Kronig and Brink's theoretical model assumes that the vertical axis is at the same temperature as the surface of the drop.

#### Experimental Cooling Curves

The heat removal rate from a cooling drop was estimated by measuring the temperature rise in the continuous phase as it passed the drop. The portion of the continuous phase heated by the drop rose in a thin column only about 4 mm. in diameter. Based on the velocity and temperature profiles in this heated column, the heat removal rate from the drop can be obtained by

$$q = 2\pi\,(\rho C_v)_c \int_o^{D_t/2} V(r)\,(T - T_\infty) r\,dr \qquad (6)$$

Since the heated column diameter was small compared to that of the tube, it could be assumed with only a 1% error that the velocity within the column was uniform and equal to the maximum velocity. An entrance effect analysis indicated that the parabolic laminar flow profile would be reestablished after a disturbance in much less distance than that between the probe and the drop.

$$V(r) \approx 2V_m = \frac{8W}{\pi D_t^2 \rho} \qquad (7)$$

Thus

$$q = \frac{16\,W\,(C_v)_c}{D_t^2} \int_o^{\frac{D_t}{2}} (T - T_\infty) r\,dr \qquad (8)$$

The temperature profiles in the heated column were constructed from a series of curves obtained by measuring the temperature decay at particular points in the heated column as the drop was allowed to cool. Such temperature decay measurements were made at points 0.5 mm. apart along a horizontal line passing through the center of the heated column.

These measured temperature profiles in the heated column were used in Equation (8) to calculate the experimental heat flow rate vs. time for the entire cooling period. The heat flow rate curves were then integrated numerically by the relationship

$$H(t) = \int_t^\infty q\,dt \qquad (9)$$

to obtain the enthalpy of the drops as a function of time. The experimental cooling curves presented as $H(t)/H(o)$ vs. dimensionless time are shown in Figure 6. In this figure the increased cooling rate of the drop with full circulation over that of the retarded drop is readily apparent.

Average initial temperatures of the drops were calculated by

$$(T_m - T_\infty)\big|_{t=0} = \frac{2H(o)}{3\pi a^3 (\rho C_v)_d} \qquad (10)$$

The calculated initial temperatures were 3.6° and 4.0°F. above the continuous phase for the cases of retarded and full circulation, respectively. These values when com-

pared to the estimate of 4.5° to 5°F. obtained by graphically integrating the temperature distributions of Figures 4 and 5 are found to be somewhat low. This indicates that the heat flow rate measurements were low, possibly as much as 25 to 35%. This deviation is not surprising, since the heat flow data were based on the measurement of temperature profiles in a heated continuous phase column only about 4 mm. in diameter. It should also be noted that $H(o)$ is calculated from the integral, Equation (9), and some error must be anticipated at large times where the drop is approaching the continuous phase temperature. However, the measured values should be proportional to the true thermal flux. For this reason the data as presented in Figure 6 as a ratio should be much more accurate than the direct measurements, and the error presumably is much less than 30%.

Because of the large transport resistance in the continuous phase in these experiments, a comparison of the experimental cooling curves with those predicted by theory is difficult. For large continuous phase resistance the shape of the theoretical cooling curves is strongly dependent on the assumed value of the external heat transfer coefficient.

Both experimental cooling curves decay in an almost exponential manner. Cooling curves based on the theoretical equations also decay in this manner for time large enough, so that the first term in the series dominates. For this reason the experimental curves could be fitted closely by any of the theoretical equations, provided the external transport coefficient was properly chosen.

It should be mentioned that the exponential shape of the curves indicates that the first term in the series of eigenfunctions is dominating. In other words, to within the precision of the measurements, the long time asymptote is approached almost as soon as the measurements are initiated. A nonuniform initial temperature distribution exists within the experimental drops, whereas a uniform initial temperature distribution is assumed in prior theoretical work. The nonuniform initial condition should have an effect on the higher order eigenfunctions, but the first eigenfunction and the long-time asymptote should be independent of the initial condition. Hence, it could be inferred that the initial condition is not important in comparisons with prior theoretical work. However, such an inference must be made with caution since the basis for the eigenfunction representation is subject to question for the case of the nonuniform interfacial temperature.

The entire experimental cooling curve for the circulating drop is closely approximated by the Kronig and Brink equation with $N_{Nu} = 62$ or by the completely mixed drop equation with $N_{Nu} = 41$. The curve cannot be approximated by the solid sphere equation, because this would require an external Nusselt number approaching infinity. The Levich correlation [Equation (5)] for the external transport coefficient for a circulating drop predicts that $N_{Nu} = 42$.

A similar comparison can be made for the retarded drop cooling curve. This curve is fitted by the solid sphere equation with $N_{Nu} = 63$, the Kronig and Brink equation with $N_{Nu} = 30$, or the completely mixed drop equation with $N_{Nu} = 25$. The Levich correlations [Equations (5) and (6)] for the external transport coefficient predict that $N_{Nu} = 40$ for a circulating drop and $N_{Nu} = 16$ for a solid sphere. Since the completely mixed drop model is the limiting case of no internal transport resistance, then $N_{Nu}$ required for a fit of this equation is a minimum value. Thus, $N_{Nu}$ cannot be as low as the value predicted by the Levich solid sphere correlation.

The comparisons given above seem to indicate that the Kronig and Brink analysis underestimates transport rates. However, it must be emphasized that the comparisons depend heavily on the transport relationship used for the continuous phase, and the influence of the initial condition has been neglected. In addition, Kronig and Brink and other earlier workers have assumed the interface to be isothermal, since this assumption makes it possible to uncouple the problems in the two phases. A theoretical program is being carried out which will extend the theory to take these differences into account and will include simultaneous solution of the energy equation in the two phases. The experimental measurements reported here will provide a detailed test of the results of the calculations.

## CONCLUSION

The new experimental technique presented here makes it possible for the first time to obtain detailed measurements of the temperature distribution in and around drops. In prior experimental work there have been well-known difficulties associated with corrections for transport during drop formation and collection, in addition to the difficulty in interpretation of changes in overall mixed mean temperature or concentration under transient conditions. These difficulties are avoided for the most part in the new technique. It is anticipated that the measurements will be useful in assessing and extending the range of validity of prior theoretical work.


## ACKNOWLEDGMENT

This work was supported by the National Science Foundation under Grant Number GK-79.


## NOTATION

$a$ = drop radius
$B_n$ = coefficient, function of $hD/k_d$
$C_v$ = specific heat
$D$ = drop diameter
$D_t$ = tube diameter
$g$ = acceleration of gravity
$h$ = continuous phase heat transfer coefficient
$H(t)$ = enthalpy of drop
$H(o)$ = initial enthalpy of drop
$k$ = thermal conductivity
$N_{Nu}$ = Nusselt number for the continuous phase, $hD/k$
$N_{Pe}$ = Peclet number, $v_\infty D/\alpha_c$
$N_{Pr}$ = Prandtl number
$N_{Re}$ = Reynolds number
$q$ = heat removal rate
$q(o)$ = initial heat removal rate
$r$ = radial distance
$t$ = time
$t^*$ = dimensionless time = $\alpha_d t/a^2$
$T$ = temperature
$T_a$ = drop surface temperature
$T$ = bulk continuous phase temperature
$v$ = velocity
$V$ = volume
$w$ = mass flow rate

### Greek Letters

$\alpha$ = thermal diffusivity, $k/\rho C_v$
$\gamma_n$ = eigenvalue, function of $hD/k_d$
$\theta$ = spherical coordinate
$\mu$ = viscosity
$\rho$ = density
$\psi$ = Hadamard stream function

### Subscripts

$c$ = continuous phase
$d$ = disperse (drop) phase
$m$ = mean value

**LITERATURE CITED**

1. Calderbank, P. H., and I. J. O. Korchinski, *Chem. Eng. Sci.*, **6**, 65 (1956).
2. "Dow Corning Silicone Notes," Bulletins No. 05-013, 05-014, and 05-015, Dow Corning Corp., Midland, Mich. (June, 1962).
3. Elzinga, E. R., Jr., and J. T. Banchero, *Chem. Eng. Progr. Symposium Ser. No. 29*, **55**, 149 (1959).
4. Head, H. N., Ph.D. thesis, Rice Univ., Houston, Tex. (1964).
5. Horton, T. J., M.S. thesis, Illinois Inst. Technol., Chicago (June, 1960).
6. Kronig, R., and J. C. Brink, *App. Sci. Res.*, **A2**, 142 (1949).
7. Levich, V. G., "Physicochemical Hydrodynamics," Prentice-Hall, Englewood Cliffs, N. J. (1962).
8. McDowell, R. V., and J. E. Myers, *A.I.Ch.E. J.*, **2**, 384 (1956).
9. Miner, C. S., and N. N. Dalton, "Glycerol," A.C.S. Monograph Ser. No. 117, Reinhold, New York (1953).
10. Pohl, H. A., *Sci. Am.*, **203**, 107 (December, 1961).



*Manuscript received July 19, 1965; revision received December 27, 1965; paper accepted January 3, 1966. Paper presented at A.I.Ch.E. San Francisco meeting.*


# Viscosity and Thermal Conductivity of Nitrogen—*n*-Heptane and Nitrogen—*n*-Octane Mixtures


**L. T. CARMICHAEL and B. H. SAGE**

**California Institute of Technology, Pasadena, California**



**Measurements of the thermal conductivity and viscosity of *n*-heptane and *n*-octane in the gas phase were made at temperatures of 100° and 160°F. and at pressures below 1 atm. In addition, measurements of the viscosity and thermal conductivity of binary gas mixtures of nitrogen and *n*-heptane were made at 160°F. at pressures below 1 atm.**


Only limited measurements of the viscosity and thermal conductivity of *n*-heptane and *n*-octane in the gas phase have been made. In the case of viscosity, these include the measurements of Lambert (*11*) and of Melaven (*13*). Moser (*14*) and Lambert (*11*) measured the thermal conductivity of these two aliphatic hydrocarbons in the gas phase. There appear to be no measurements of the viscosity or thermal conductivity of mixtures of these hydrocarbons with nitrogen or air.

The evaporation of *n*-heptane (*1, 2, 10*) and *n*-octane (*20*) into turbulent air streams has been studied in the course of experimental work on the material transport from spheres. In the analysis of the results, specific information concerning the viscosity and thermal conductivity of mixtures of these hydrocarbons with air was desirable. The available methods of predicting the viscosity and thermal conductivity of mixtures (*3, 12, 21*) are based primarily on the Chapman-Enskog theory (*9*) which is applicable to monatomic spherical species of molecular weights which do not differ markedly. Since the analysis of turbulent transport in air streams depends upon a knowledge of the transport properties of mixtures, limited measurements were made of the thermal conductivity and viscosity of binary gas mixtures of *n*-heptane with nitrogen at pressures between atmospheric and attenuation away from the dew point.

## MIXTURE RULES

Chapman and Enskog (*9*) developed basic principles for behavior of mixtures of monatomic species involving spherical molecules in mixtures where the nature of the properties and molecular weights of each of the species do not differ greatly. Lindsay and Bromley (*12*) have suggested a mixture rule of the following form:

$$k_m = \frac{k_1}{1 + A_1(n_2/n_1)} + \frac{k_2}{1 + A_2(n_1/n_2)} \qquad (1)$$

where

$$A_1 = \frac{1}{4}\left\{ 1 + \left[\frac{\eta_1}{\eta_2}\left(\frac{M_2}{M_1}\right)^{3/4} \frac{1 + (S_1/T)}{1 + (S_2/T)}\right]^{1/2}\right\}^2 \frac{1 + (S_{12}/T)}{1 + (S_1/T)} \qquad (2)$$

$A_2$ corresponds to $A_1$ with the subscripts interchanged. Similar expressions may be used for viscosity (*21*). Under the circumstances where $A_1$ and $A_2$ are unity, Equation (1) corresponds to a linear variation in the thermal conductivity or viscosity with mole fraction of the component. In the case where $A_1 = M_2/M_1$ and $A_2 = M_1/M_2$, a linear variation with weight fraction results: